Surface plasmons at the Brillouin zone boundary of an oblique lattice

Thomas J. Constant, Pete Vukusic, Alastair P. Hibbins, and J. Roy Sambles

Citation: Appl. Phys. Lett. **106**, 091106 (2015); doi: 10.1063/1.4914479
View online: https://doi.org/10.1063/1.4914479
View Table of Contents: http://aip.scitation.org/toc/apl/106/9
Published by the American Institute of Physics

Surface plasmons at the Brillouin zone boundary of an oblique lattice

Thomas J. Constant,[a] Pete Vukusic, Alastair P. Hibbins, and J. Roy Sambles
Department of Physics and Astronomy, University of Exeter, Stocker Road, Exeter, Devon EX4 4QL, United Kingdom

(Received 27 January 2015; accepted 28 February 2015; published online 6 March 2015)

In periodic systems of low-symmetry, the Bragg condition for the complete interference of waves along the contour of the Brillouin zone (BZ) boundary is not generally satisfied. As a result, band-gaps do not necessarily occur at this boundary. This letter demonstrates this experimentally by recording the iso-frequency contours for surface plasmon polaritons (SPPs) supported on a diffraction grating with an underlying 2D oblique Bravias lattice. It is shown that these contours do not intersect the BZ boundary perpendicularly, as the symmetry operations of the lattice place no conditions on the surface wave interference at this boundary. © *2015 AIP Publishing LLC*.
[http://dx.doi.org/10.1063/1.4914479]

From polaritons in photonic thin-films and phonons in acoustic metamaterials to spin-waves in magnetic media and electrons in crystals, the interaction and formation of stationary waves at Brillouin zone (BZ) boundaries are a phenomena that permeate many active areas of modern physics.

Recently, there has been huge interest in the formation of standing waves in 2D systems, spurred on by the isolation of graphene in 2004 and its associated electron transport character. The unique properties of wave propagation in the honeycomb 2D lattice of graphene have inspired work with particle plasmon lattices[1] and acoustic wave propagation.[2] Fundamental to all these standing wave studies, and the possible formation (or denial) of band-gap formation, is the periodic lattice through which these elementary oscillations travel.

In this letter, it is experimentally demonstrated that the formation of band-gaps on an oblique lattice does not occur at the BZ boundary, which is a consequence of the lattice symmetry.

The wave used for this investigation is a surface plasmon polariton (SPP) supported on a diffraction grating that provides the underlying oblique lattice. An oblique lattice is formed of an infinite array of lattice points separated by two lattice vectors of different magnitudes, oriented at an angle with respect to each other (α), such that $\alpha \neq 90°$. To realise this symmetry using surface-relief gratings, two diffraction gratings of different pitches are "crossed" at an angle α such that $\alpha \neq 90°$, forming an oblique bigrating. Such a grating is illustrated in Figure 1(a).

The reciprocal space map of the corresponding lattice is shown in Figure 1(b) and constitutes the lowest symmetry lattice set of all the two-dimensional Bravais lattices. This reciprocal lattice is itself oblique, with the reciprocal lattice vectors defined as $\mathbf{k}_{gx}$ and $\mathbf{k}_{gv}$, oriented at an angle $\alpha^{\star} = 180° - \alpha = 105°$ with respect to each other. The only symmetry operation possible for this oblique lattice is a rotation around a lattice point of 180°, which for 2D lattices is the equivalent of an inversion operation. Centred about each lattice point in Figure 1(b) are circles representing various scattered iso-frequency contours. The circles formed with solid lines show the contours for a grazing photon, and the dashed lines represent the iso-frequency contours for scattered SPPs which lie outside their respective grazing-photon lines (diffraction lines) due to the greater momentum of SPPs compared to light. In this simple cartoon, the SPPs do not interact and cross through each other unperturbed. However, if the SPPs interact to form band-gaps these iso-frequency contours will deform.[3] The black circle is the case of the un-scattered zero-order light, which is the region of *k*-space accessible for mapping using the experimental method of imaging scatterometry.[4]

To realise an underlying oblique lattice along which the surface waves propagate, SPP supporting bigratings were fabricated. The coordinate system for this type of grating is

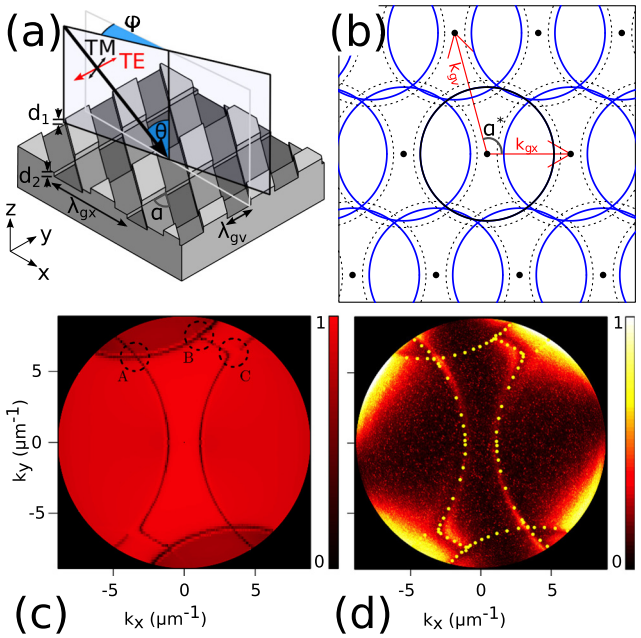

FIG. 1. (a) A schematic of the oblique bigrating and the coordinate system. (b) The corresponding reciprocal space map of the oblique lattice with solid/dotted line circles indicating scattered light/SPP momentum states at a fixed frequency. (c) Modelled and (d) experimentally mapped iso-frequency contours via reflection (colorscale) of SPs on an oblique lattice. The mode minima from (a) have been included in (d) as yellow circles for comparison.

[a]Electronic mail: t.j.constant@exeter.ac.uk

shown in Figure 1(a). The plane of incidence is defined at an azimuthal angle of ϕ so that when $\phi = 0°$ the wavevector of incidence light lies along the x-direction. When the electric field vector of the impinging radiation is contained within the plane of incidence, the light is said to be TM polarised, and when the electric vector lies orthogonal to the plane, it is TE polarised. The x-direction is collinear with the grating vector $\mathbf{k}_{gx} = 2\pi\hat{\mathbf{x}}/\lambda_{gx}$ for the longer-pitch grating, which possesses a periodicity of λ_{gx}. This period, for all the gratings presented in this letter, is $\lambda_{gx} = 600$ nm. The second, shorter-pitch grating lies at an angle of $\alpha = 75°$ along the v axis (defined lying in the xy plane at an angle α to $\hat{\mathbf{x}}$) and for the grating presented in this letter has a period $\lambda_{gv} = 400$ nm. The grating vector of this short-pitch grating is defined as $\mathbf{k}_{gv} = 2\pi\hat{\mathbf{v}}/\lambda_{gv}$. An angle of $\alpha = 75°$ was chosen to lie midway between the high symmetry cases of $\alpha = 60°$ (hexagonal-like) and $\alpha = 90°$ (square/rectangular). The ratio of grooves to pitch of the gratings is designed as $\Gamma_x = \Gamma_v = 0.5$. The depths of the gratings are d_1 and d_2, and are designed as $d_1 = d_2 \approx 40$ nm. The gratings for this letter were fabricated using electron beam lithography (EBL) and a template stripping method.[5]

The iso-frequency contours of SPPs are mapped using imaging scatterometery.[4] In this technique, reflectivity anomalies map the allowed momentum contours of the SPP modes. Figure 1(c) shows theoretical iso-frequency contours for an oblique bigrating at $\lambda_0 = 700$ nm. The corresponding experimentally obtained iso-frequency surface is shown in Figure 1(d). In the experimental plot at the illuminating wavelength of 700 nm, the contrast of the entire SPP contour to the background is weak, making the determination of the mode position in k-space difficult. To improve the contrast, the polarisers of the scatterometer are crossed, producing a dark background reflectivity against which the polarisation conversion mediated by the SPPs[6] provides greater contrast for the mode positions. The four bright lobes of high reflectivity are polarisation conversion mediated by the ellipsoidal mirror in the apparatus.

The numerical prediction for the same system shown in Figure 1(c) is obtained using the Chandezon method,[7] approximating the square groove profiles with the Fourier sums, $F(x,v) = \sum_{n=1,3} \frac{4A}{n\pi} \cos \frac{2n\pi x}{\lambda_{gx}} + \sum_{n=1,3} \frac{4A}{n\pi} \cos \frac{2n\pi v}{\lambda_{gv}}$, which provide a suitable approximation to a lamella bi-grating with a depth of $2A = 40$ nm, $\lambda_{gx} = 600$ nm, $\lambda_{gv} = 400$ nm, $\alpha = 75°$, and a ratio groove to pitch spacing of $\Gamma = 0.5$. The dielectric function of silver is taken from literature,[8] and for the illuminating wavelength of 700 nm is equal to $\varepsilon = -23.13 + 0.59i$. The light in the theoretical plot is TM polarised for every azimuthal angle. Only the $n = 1, 3$ components are included in the calculation, as the even components are considered to be absent for a grating with $\Gamma = 0.5$. The modelled values for the mode position (taken from the theoretical plot at the position of reflectivity minima) found in Figure 1(c) are plotted on the experimental results from Figure 1(d) as yellow circles, and show excellent agreement. This agreement justifies the assumption that the dominant scattering amplitudes in the observable SPP band structure are only the $n = 1, 3$ components.

When a SPP meets an equivalent counter-propagating SPP a standing wave forms, there are generally two possible arrangements of the electric field for this SPP standing wave on a grating, which will generally differ in energy. This leads to an upper and lower energy band, with an energy range between them where SPP propagation is forbidden.[9] The energy gap size is dependent on the energy of the two possible field distributions and so is linked intimately to the surface geometry. The surface profile also provides the scattering mechanism by which SPPs Bragg scatter to meet counter-propagating SPPs and form these standing waves. The strength of this scattering and so the amplitude of the Bragg scattered SPP affect the size (in frequency) of the band-gap.[9]

In the upper half-space of Figure 1(c), three SPP mode crossings are labelled A–C. Crossing point A is the meeting of a (−1, 0) and a (0, 1) Bragg scattered SPP contour. These two SPP curves are separated in k-space by a minimum of two scattering vectors, and so require a multiple scattering process to interact with each other. With no 2nd order harmonics in the grating profile, the interaction is weak and no band-gap is observed. The crossing point B is the intersection of the (0, 1) and (1, 1) SPPs. This is a process by which the SPPs must scatter a total of 1 $\mathbf{k}_{gx}$ to interact, and so a small band-gap forms. At point C, the (1, 0) and (1, 1) SPP cross. These are separated by a single scattering vector 1 $\mathbf{k}_{gv}$, and so interact, forming a large band-gap.

In this paragraph, we present results that show that on a surface with such low symmetry the locations in k-space of SPP standing waves do not necessarily occur at the BZ boundary. This concept is known for the band-gaps that occur for electron propagation in crystals,[10] and is demonstrated here for surface waves on a periodic lattice. To show this clearly, we must identify how plasmonic band-gaps are illustrated in the iso-frequency contours recorded with imaging scatterometry. The iso-frequency image obtained using scatterometry maps k-space at a single frequency, with SPP bands seen as an anomaly in the reflected light. The group velocity of a general propagating wave is defined as, $\mathbf{v}_g = \nabla_k\, \omega(\mathbf{k})$, where $\mathbf{v}_g$ is the group velocity, $\omega(\mathbf{k})$ is the angular frequency of the wave as a function of wavevector, $\mathbf{k}$, and ∇_k is the gradient operator with respect to k. For a small change in frequency $d\omega$, the corresponding small movement in k-space, $d\mathbf{k}$, is related to this group velocity simply by $d\omega = \nabla_k\, \omega(\mathbf{k}) \cdot d\mathbf{k}$. For an iso-frequency contour, there must be no change in frequency along the contour ($d\omega = 0$). Setting $d\omega = 0$ restricts the values of $d\mathbf{k}$ to those values that move along a contour of equal frequency. It is then apparent since $\mathbf{v}_g \cdot d\mathbf{k} = 0$, $\mathbf{v}_g$ must lie perpendicular to $d\mathbf{k}$. This is true for any general contour of constant frequency. If the group velocity in one direction falls to zero at a boundary, such as at the BZ boundary, the iso-frequency SPP contour will intersect that boundary perpendicularly.

Figure 2 shows the mapped iso-frequency contours of SPPs for the oblique grating at a wavelength of $\lambda_0 = 650$ nm. The position of the SPP contours are found to present as bands of low reflectivity, with the polariser of the experiment chosen in this case to best couple light to the (±1, 0) modes. Also annotated on the figure are the diffracted light circles (blue lines) and the BZ boundary formed using the Wigner-Seitz method[11] (green line).

It is observed that the SPP contour passes through the BZ boundary seemingly unperturbed. In Figure 2, the SPP contour following the (−1, 0) diffracted light circle is shown

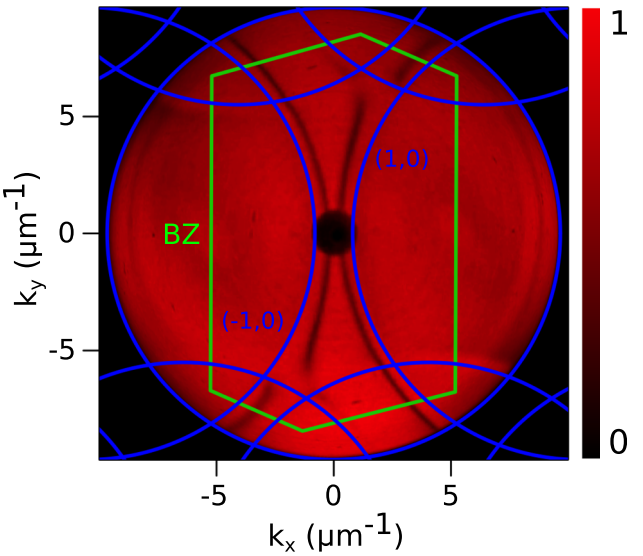

FIG. 2. Experimentally mapped surface plasmon iso-frequency contour via reflectivity (colorscale) at $\lambda_0 = 650$ nm passing through the first BZ boundary. This contour neither meets the boundary perpendicularly nor is perturbed as it passes through, showing that the group velocity of the SP mode is still finite across the boundary.

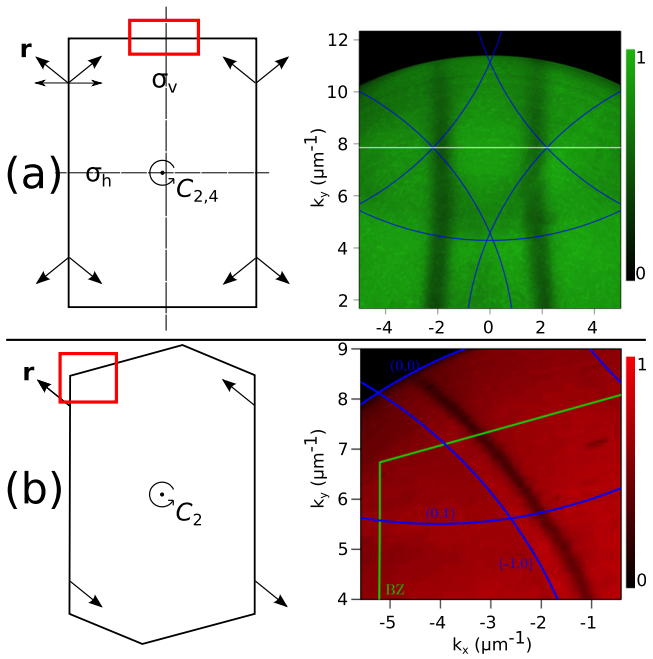

FIG. 3. (Left) The BZ boundary of a (a) rectangular lattice and (b) and oblique lattice. The symmetry operations labelled allow the deduction of the shown vectors (arrows) from a single unit vector, **r**. (Right) Measured SPP iso-frequency contours around the BZ boundary (indicated by the red squares, (left) for (a) a rectangular lattice at $\lambda_0 = 550$ nm and (b) the oblique lattice at $\lambda_0 = 650$ nm.

to pass through the BZ at an angle which is not perpendicular to the boundary. This means that at the boundary, the SPP's group velocity in the (0, 1) direction is not zero, and no standing-wave states in this direction have formed. The (0, 1) scattered SPP is not observed in this figure as the polarisation of the illuminating light has been chosen to only couple strongly to the (1, 0) SPP. Additionally, the (−1, 0) and (uncoupled) (0, 1) SPPs are not seen to interact, separated as they are by a weak multiple scattering process.

An example of SPP contours intersecting the BZ boundary on a rectangular lattice is shown for comparison in Figure 3(c). This scattergram is taken from a plasmonic grating with rectangular symmetry previously published in Ref. 4, at a wavelength of 550 nm. The visible dark bands correspond to the momentum states of the (±1, 0) scattered SPPs, and are highly perturbed from their corresponding (±1, 0) light lines, constrained as they are to meet this boundary perpendicularly. Such perturbations of SPP contours at the BZ boundary have also been observed for hexagonal[12] and square[13] symmetry lattices.

A Brillouin zone boundary in reciprocal space outlines a primitive unit cell in the reciprocal lattice and contains on the boundary points of high-symmetry. To determine this boundary that contains the maximum amount of high-symmetry points, the perpendicular bisectors of the vectors connecting the nearest neighbours to one lattice point are drawn, a method known as the Wigner-Seitz method.[11] For the highly symmetric cases of square, rectangular, or hexagonal lattices, the boundary is a constant contour of high symmetry.

Neumann's principle with respect to our system requires that the physical properties of phenomena associated with the grating possess the same symmetry as the point symmetry group of the grating.[14] Figure 3(a) shows an arbitrary vector, **r** lying on the boundary of a rectangular unit cell. In the case of a rectangular grating, the mirror and translational symmetry allows the deduction of the other shown vectors through various reflections in the σ_v and σ_h planes or rotations about the C point. These vectors sum to give a magnitude of zero in the direction perpendicular to the zone boundary. Whether this vector field represents the SPP's momentum, group velocity, or Poynting vector, the conclusion is the same: a standing wave forms perpendicular to the BZ boundary. These are observed experimentally as discontinuities of the SPP curves at the BZ boundary.

Using the same approach, we apply the symmetry operations of the oblique lattice to an arbitrary vector field in Figure 3(b). With no mirror symmetry, the oblique lattice possesses only translational and a two-fold rotation symmetry operations. As shown in the figure, there are no special conditions on the vectors lying along the BZ boundary formed using the Weigner-Seitz method, and no condition for the vectors to cancel perfectly. Standing waves do not necessarily occur at the BZ boundary. Notice that where SPPs meet at other locations inside the unit cell (see Figure 2) they do form band-gaps, but there is no requirement from symmetry that these intersections occur at the BZ boundary. This condition has recently been found in a theoretical study of acoustic waves in 2D phononic crystals.[15]

In conclusion, SPPs propagating on an oblique bigrating have been investigated. The dispersion of these surface modes has been mapped experimentally and the SPP interactions discussed in terms of the available scattering amplitudes of the grating. Using imaging scatterometry, it is observed that the SPP contours are not perturbed as they pass through the conventional BZ boundary. A generalized discussion on the symmetry of the BZ is presented, concluding that this is because the BZ boundary on an oblique grating is not a contour of high symmetry, and only contains

isolated points around which the symmetry conditions may be met for the formation of SPP standing waves. The experimental results are supported by excellent agreement with numerical predictions.

Sponsorship for this work was received from the EPSRC (Grant No. EP/G022550/1), HP Labs Bristol, and the USAF (Award No. FA9550-10-1-0020).

[1]G. Weick, C. Woollacott, W. Barnes, O. Hess, and E. Mariani, "Dirac-like plasmons in honeycomb lattices of metallic nanoparticles," Phys. Rev. Lett. **110**, 106801 (2013).
[2]J. Lu, C. Qiu, S. Xu, Y. Ye, M. Ke, and Z. Liu, "Dirac cones in two-dimensional artificial crystals for classical waves," Phys. Rev. B **89**, 134302 (2014).
[3]R. A. Watts, J. Harris, A. Hibbins, T. Preist, and J. R. Sambles, "Optical excitation of surface plasmon polaritons on 90 and 60 bi-gratings," J. Mod. Opt. **43**, 1351–1360 (1996).
[4]T. J. Constant, A. P. Hibbins, A. J. Lethbridge, J. R. Sambles, E. K. Stone, and P. Vukusic, "Direct mapping of surface plasmon dispersion using imaging scatterometry," Appl. Phys. Lett. **102**, 251107 (2013).
[5]T. J. Constant, "Optical excitation of surface plasmon polaritons on novel bigratings," Ph.D. thesis, University of Exeter, 2013.
[6]G. P. Bryan-Brown, J. R. Sambles, and M. C. Hutley, "Polarisation conversion through the excitation of surface plasmons on a metallic grating," J. Mod. Opt. **37**, 1227–1232 (1990).
[7]J. Chandezon, D. Maystre, and G. Raoult, "A new theoretical method for diffraction gratings and its numerical application," J. Opt. (Paris) **11**, 235–241 (1980).
[8]D. J. Nash and J. R. Sambles, "Surface plasmon-polariton study of the optical dielectric function of silver," J. Mod. Opt. **43**, 81–91 (1996).
[9]W. L. Barnes, T. W. Preist, S. C. Kitson, and J. R. Sambles, "Physical origin of photonic energy gaps in the propagation of surface plasmons on gratings," Phys. Rev. B **54**, 6227–6244 (1996).
[10]P. G. Radaelli, "Lecture 4—Symmetry in the solid state - Part IV: Brillouin zones and the symmetry of the band," 2012.
[11]C. Kittel and P. McEuen, *Introduction to Solid State Physics* (Wiley New York, 1996), vol. 7.
[12]C. J. Regan, A. Krishnan, R. Lopez-Boada, L. Grave de Peralta, and A. A. Bernussi, "Direct observation of photonic Fermi surfaces by plasmon tomography," Appl. Phys. Lett. **98**, 151113 (2011).
[13]C. J. Regan, L. Grave de Peralta, and A. A. Bernussi, "Equifrequency curve dispersion in dielectric-loaded plasmonic crystals," J. Appl. Phys. **111**, 073105 (2012).
[14]R. E. Newnham, *Properties of Materials: Anisotropy, Symmetry, Structure* (Oxford University Press, Oxford, 2005).
[15]J. Hu and W. Xu, "The Brillouin zones and band gaps of a two-dimensional phononic crystal with parallelogram lattice structure," Sci. China Phys. Mech. **57**, 1–7 (2014).